Systematic study of carrier correlations in the electron-hole recombination dynamics of quantum dots

T. Berstermann, T. Auer, H. Kurtze, M. Schwab, D. R. Yakovlev, and M. Bayer
Experimentelle Physik II, Universität Dortmund, 44221 Dortmund, Germany

J. Wiersig, C. Gies, and F. Jahnke
Institute for Theoretical Physics, University of Bremen, 28334 Bremen, Germany

D. Reuter and A. D. Wieck
Angewandte Festkörperphysik, Ruhr-Universität Bochum, D-44780 Bochum, Germany
(Received 25 June 2007; revised manuscript received 1 October 2007; published 26 October 2007)

The ground state carrier dynamics in self-assembled (In,Ga)As/GaAs quantum dots has been studied using time-resolved photoluminescence and transmission. By varying the dot design with respect to confinement and doping, the dynamics is shown to follow in general a nonexponential decay due to carrier correlations. Only for specific conditions in regard to optical excitation and carrier population, for example, can the decay be well described by a monoexponential form. For resonant excitation of the ground state transition, a strong shortening of the luminescence decay time is observed as compared to the nonresonant case. The results are consistent with a microscopic theory that accounts for deviations from a simple two-level picture.

DOI: 10.1103/PhysRevB.76.165318 PACS number(s): 42.25.Kb, 78.55.Cr, 78.67.De

I. INTRODUCTION

The carrier recombination dynamics in semiconductor quantum dots (QDs) is typically analyzed in terms of exponential decays with a characteristic time constant τ in which all possible decay channels are comprised by adding the corresponding decay rates to give the total decay rate $1/\tau$. This kind of decay has been adopted from experiments in atomic physics, which are discussed using two-level schemes corresponding to the following scenario: An electron has been excited to a higher lying atom shell, from which it relaxes to a vacancy in a lower lying shell. In many cases, the relaxation is dominated by radiative recombination, for which monoexponential decays give an appropriate description of the relaxation process.

Due to the three-dimensional confinement of carriers, semiconductor QDs resemble the solid state analog of atoms. This has been underlined by the demonstration of effects observed before in atom optics such as a radiatively limited spectral linewidth,[1] antibunching in the photon emission statistics,[2] a square-root power broadening for resonant excitation,[3] etc. Most of these results were obtained at cryogenic temperatures. At elevated temperatures, the scattering of confined carriers with lattice phonons, for example, becomes strong, as manifested by a strong broadening of the optical transitions.[4] To some extent, this broadening resembles the collision induced broadening of optical transitions in high pressure atom gases.

Furthermore, experiments addressing electron-hole recombination in semiconductors are often performed in a way that not only two electronic levels are involved. Instead, a pulsed laser excites carriers nonresonantly above the barrier, from where they are captured by the confinement potential and relax toward the QD ground state. This situation can be thought to be analogous to a situation in which the atoms have been ionized to a plasma of electrons and ions. During plasma cooling, the electrons are trapped by the ions and relax by photon emission.

Under such conditions, the carrier dynamics, in general, cannot be described by a monoexponential decay, in agreement with many observations reported in literature for QD ensembles. On the other hand, there have been reports about exponential decays in such ensemble studies.[5] Also for single QD experiments, indications for a nonexponential dynamics have been found.[6] The observed nonexponentiality has been ascribed to various origins such as carrier diffusion to the QDs,[5,7] state filling effects due to Pauli blocking,[5,8,9] inhomogeneities concerning electron-hole overlap,[10–15] confinement potential fluctuations from quantum confined Stark effect due to charges in the QD vicinity,[16] as well as formation of optically inactive excitons with parallel electron and hole spins.[11,17] All these factors may be of relevance for particular experimental situations.

However, many studies have been done for specific situations regarding the QD properties, from which it is hard to develop a systematic picture. Here, we have performed time-resolved studies of the carrier dynamics, covering a wide range of parameters with respect to these properties such as confinement potential height and residual carrier population. In addition, the optical excitation conditions were chosen such that many of the factors mentioned above can be ruled out. For example, the excitation power was chosen so low that multiexciton effects due to state filling were very rare. The influence of carrier diffusion was ruled out by comparing excitation above the barrier to excitation below the barrier. By doing so, also the influence of the environment on the confinement potential shape was under control.

As a result, we present in the following a detailed analysis of the dynamics of carriers in the QD exciton ground state. We show that decays which are to a good approximation monoexponential can occur, but only under very specific conditions such as fully resonant excitation or very strong

QD confinement. Under other circumstances, nonexponential decays are found. Interestingly, strictly resonant excitation also leads to a pronounced enhancement of the carrier recombination rate.

The paper is organized as follows. In the next section, we briefly discuss the theory of QD photoluminescence,[18] which is used to analyze the subsequent experimental studies. In Sec. III, details of the structures under study are given together with a description of the experimental techniques. The experimental data are presented and discussed in Sec. IV and the comparison with the numerical results is provided in Sec. V.

II. THEORY

In our case, the dynamics of electrons and holes in QDs was studied by two different spectroscopic techniques: time-resolved photoluminescence and time-resolved transmission. We assume that the carriers quickly lose coherence after their generation by pulsed laser excitation, e.g., by relaxation, so that we address only incoherent electron and hole populations.

(i) The intensity $I(\omega)$ in time-resolved photoluminescence (TRPL) experiments is given by the temporal evolution of the number of photons from electron-hole recombination at the detection frequency ω,

$$I(\omega) = \frac{d}{dt}\sum_{\xi} \langle b_{\xi}^{\dagger} b_{\xi}\rangle|_{|\mathbf{q}|=\omega/c}, \tag{1}$$

where $b_{\xi}^{\dagger}$ and b_{ξ} are the creation and annihilation operators of a photon in state ξ, which is characterized by the wave vector $\mathbf{q}$ and the polarization vector. The brackets $\langle\cdots\rangle$ symbolize the quantum mechanical operator averages.

(ii) A second, independent method, which allows one to draw conclusions about the dynamics of the electron and hole populations is time-resolved differential transmission (TRDT). The electron and hole populations are described by the expectation values $f_{\nu}^{e}=\langle e_{\nu}^{\dagger} e_{\nu}\rangle$ and $f_{\nu}^{h}=\langle h_{\nu}^{\dagger} h_{\nu}\rangle$, respectively. Here, $e_{\nu}^{\dagger}$ and e_{ν} ($h_{\nu}^{\dagger}$ and h_{ν}) are the creation and annihilation operators of an electron (hole) in a state ν, including the QD shell index and the spin orientation.

In the following, we are interested in the interplay of photon and population dynamics due to spontaneous recombination,

$$\frac{d}{dt}\langle b_{\xi}^{\dagger} b_{\xi}\rangle = \frac{2}{\hbar}\,\mathrm{Re}\sum_{\nu} g_{\xi\nu}^{*}\langle b_{\xi}^{\dagger} h_{\nu} e_{\nu}\rangle, \tag{2}$$

$$\frac{d}{dt} f_{\nu}^{(e,h)}|_{\mathrm{opt}} = -\frac{2}{\hbar}\,\mathrm{Re}\sum_{\xi} g_{\xi\nu}^{*}\langle b_{\xi}^{\dagger} h_{\nu} e_{\nu}\rangle. \tag{3}$$

The carrier populations are also subject to carrier-carrier Coulomb interaction[19] and to carrier-phonon interaction.[20] The dynamics of both photon and carrier population are determined by the interband photon-assisted polarization $\langle b_{\xi}^{\dagger} h_{\nu} e_{\nu}\rangle$ and its complex conjugate $\langle b_{\xi} e_{\nu}^{\dagger} h_{\nu}^{\dagger}\rangle$. The former describes the emission of a photon due to recombination of an electron-hole pair, while the latter describes the inverse process, creation of an electron-hole pair via photon absorption. The strength of the interband photon-assisted polarization is determined by the coupling matrix element of the electron-hole transition to the electromagnetic field, $g_{\xi\nu}$.

For solving Eqs. (2) and (3), the interband polarization needs to be known, which is given by its free evolution, by dephasing, by excitonic contributions, by stimulated emission (in the case of QDs embedded into a microcavity[21,22]), and by spontaneous emission, for which the source term is

$$i\sum_{\alpha} g_{\xi\alpha}\langle e_{\alpha}^{\dagger} e_{\nu} h_{\alpha}^{\dagger} h_{\nu}\rangle. \tag{4}$$

The corresponding equation of motion for this four-particle operator contains averages of six-particle operators, and so on. This is a manifestation of the well-known hierarchy problem of many-particle physics. A consistent truncation scheme is the cluster expansion,[23] where all occurring operator expectation values are represented by possible factorizations plus correlations. In our particular case, we use

$$\begin{aligned}\langle e_{\alpha}^{\dagger} e_{\nu} h_{\alpha}^{\dagger} h_{\nu}\rangle &= \langle e_{\alpha}^{\dagger} e_{\nu}\rangle\langle h_{\alpha}^{\dagger} h_{\nu}\rangle\delta_{\alpha\nu} + \delta\langle e_{\alpha}^{\dagger} e_{\nu} h_{\alpha}^{\dagger} h_{\nu}\rangle \\ &= f_{\nu}^{e} f_{\nu}^{h}\delta_{\alpha\nu} + C_{\alpha\nu\alpha\nu}^{x},\end{aligned} \tag{5}$$

where $C_{\alpha\nu\alpha\nu}^{x}=\delta\langle e_{\alpha}^{\dagger} e_{\nu} h_{\alpha}^{\dagger} h_{\nu}\rangle$ is a measure of how strongly the electron-hole pairs are correlated. In the cluster expansion method, equations of motion for the correlation contributions are derived. Then, the hierarchy of correlation contributions is truncated rather than the hierarchy of expectation values itself. This allows for the consistent inclusion of correlations in the equations of motion up to a certain order in all of the appearing operator expectation values.

In this paper, we use the above discussed theory in two different ways. For the numerical results presented in Sec. V, we solve the complete set of equations, which is consistently truncated on the doublet level (i.e., two-particle correlations due to Coulomb and light-matter interaction are included) as described in Ref. 18. To gain further insight into the physics and provide more intuitive explanations, we discuss in the remaining part of this section further analytical simplifications. A closed equation of motion for the carrier population can be obtained from the adiabatic solution of the equation for the interband photon-assisted polarization. The latter takes a simpler form when excitonic exchange effects are neglected. (In the numerical evolution, they are of course included.) This leads to[18,24]

$$\frac{d}{dt} f_{\nu}^{(e,h)}|_{\mathrm{opt}} = -\frac{f_{\nu}^{e} f_{\nu}^{h} + \sum_{\alpha} C_{\alpha\nu\alpha\nu}^{x}}{\tau_{\nu}}, \tag{6}$$

with the Wigner-Weißkopf decay rate

$$\frac{1}{\tau_{\nu}} = -\frac{2}{\hbar}\lim_{\Gamma\to 0^{+}}\mathrm{Re}\sum_{\xi}\frac{i|g_{\xi\nu}|^{2}}{\hbar\omega_{\nu}^{e} + \hbar\omega_{\nu}^{h} - \hbar\omega_{\xi} - i\Gamma}. \tag{7}$$

As a further simplification, we consider in the next two paragraphs only *s*-shell populations and one spin degree of freedom of the carriers. The carrier configuration can then be expanded into the basis set $|n_e, n_h\rangle$, where the n_e and n_h give the number of electrons and holes, respectively (the photonic

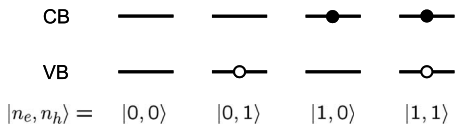

FIG. 1. Possible carrier configurations in the conduction and valence band QD ground states. The spin degree of freedom is neglected.

part of the states is of no relevance here and not shown). The possible configurations are $|0, 0\rangle$, $|0, 1\rangle$, $|1, 0\rangle$, and $|1, 1\rangle$ as displayed schematically in Fig. 1.

If the electron and hole populations were fully correlated, only $|0, 0\rangle$ and $|1, 1\rangle$ out of these four configurations would be relevant. Using the following relations for the electron and hole number operators, $e^\dagger e|0,0\rangle = h^\dagger h|0,0\rangle = 0$ and $e^\dagger e|1,1\rangle = h^\dagger h|1,1\rangle = |1,1\rangle$, we see that in this *two-level case* $\langle e^\dagger e h^\dagger h\rangle$ reduces to $f^e = \langle e^\dagger e\rangle$ and also $f^h = \langle h^\dagger h\rangle$. In this particular situation, the source term of spontaneous emission $f^e f^h + C^x = \langle e^\dagger e h^\dagger h\rangle$ in Eq. (6) can be replaced by $f^{(e,h)}$, and then the equations of motion give a single-exponential decay of the populations and correspondingly of the photoluminescence. As soon as the other two configurations are included, Eq. (6), in general, results in a nonexponential decay. In Sec. V, we evaluate C^x under more general conditions including Coulomb and carrier-photon interaction.

III. SAMPLES AND EXPERIMENT

The experiments were performed on different types of self-assembled (In,Ga)As/GaAs QD arrays fabricated by molecular beam epitaxy. All samples contained 20 layers of QDs, which were separated from one another by 60-nm-wide barriers. The first type of QDs was nominally undoped, whereas the other two types were modulation doped, one of *n* type and the other one of *p* type. The silicon- or carbon-doping sheets were located 20 nm below each dot layer. The dopant density was chosen about equal to the dot density in each layer so that an average occupation by a single electron or hole per dot can be expected.

The photoluminescence emissions of the as-grown QD samples are located around 1200 nm at cryogenic temperatures for the three dot types. In order to vary the confinement potential, several pieces from each QD sample type were thermally annealed for 30 s at different temperatures T_{ann} between 800 and 980 °C. Because of the annealing, the confinement is reduced due to intermixing of dot and barrier material. The dot base diameter is about 25 nm and the height is 5 nm for the as-grown dot sample, and these parameters are increased further by the thermal annealing. Typical photoluminescence spectra of the nominally undoped samples, which show the established behavior for such a series of annealed QD structures, can be found in Ref. 25. Increasing T_{ann} results in a blueshift as well as a narrowing of the emission line from the ground state exciton. The corresponding blueshift of the wetting layer is found to be rather weak as compared to that of the QD emission. Therefore, the confinement potential, which we define as the energy separation between the wetting layer emission and the QD ground state emission, varies systematically within an annealing series. The confinement energies decrease from about 400 down to 50 meV with increasing T_{ann}.

The QD samples were mounted on the cold finger of a microscopy flow cryostat which allows temperature variations down to 6 K. In the TRPL studies, a mode-locked Ti-sapphire laser emitting linearly polarized pulses with a duration of about 1 ps at 75.6 MHz repetition rate (corresponding to 13.2 ns pulse separation) was used for optical excitation. The QD luminescence was dispersed by a monochromator with 0.5 m focal length and detected by a streak camera with an S1 photocathode. In the standard synchroscan configuration, time ranges up to 2 ns could be scanned with a resolution of about 20 ps. Longer time ranges could be addressed by installing a long delay time unit, reducing the time resolution to ~50 ps. The excitation was kept as weak as possible to avoid multiexciton effects (see below).

In the TRDT studies, two synchronized Ti-sapphire lasers with a jitter well below 1 ps were used for excitation. The emission energies could be varied independently. One laser beam, the pump, was used for the creation of carrier populations, while the other one, the probe, was used to test them. The temporal delay between both pulses could be varied by a mechanical delay line, along which the pump beam was sent. The transmission of the probe was detected with a homodyne technique based on phase-sensitive balanced detection. The polarization of the pump and of the probe beam were chosen either linearly or circularly copolarized.

We mention already here that the main topic of our studies is not the quantitative values of the decay times, which have been addressed already in many other studies. The focus is instead to develop a systematic picture of the dependence of the recombination on experimental parameters, both the internal QD properties and the external conditions such as excitation energy and intensity.

For clarity, we discuss the relation of time-resolved studies on an array of QDs (as in our case) and on a single QD. Obviously, single dot measurements do not suffer from inhomogeneities related with dot geometry or composition, which are translated into variations of the dipole transition matrix elements. Due to these variations, the ensemble dynamics is given by a superposition of transitions with different matrix elements. Even though one expects therefore an intrinsic nonexponentiality, exponential decays have been reported,[5] most likely because deviations are smeared out in the superposition leading to an effective averaging (in addition to potential charged exciton contributions, see below). Still, a systematic variation of experimental conditions as done here allows one to obtain detailed information about the influence of carrier correlations on the decay form.

On the other hand, in order to obtain enough signal strength, single dot measurements typically have to be integrated over many more pulsed excitation cycles than in ensemble measurements. During the long integration time, many factors which determine the decay may vary such as carrier diffusion for above-barrier excitation, confinement potential due to environmental charges, etc. All these factors will lead also to observation of an averaged decay.

IV. RESULTS AND DISCUSSION

The outline of the carrier recombination dynamics in Sec. II provides a guide for the experimental studies. An exponential decay could occur if the carrier populations were fully correlated, i.e., excitonic correlations were present. However, in experiments, in which the carriers are created by nonresonant excitation into the wetting layer or the barrier, electrons and holes typically relax independently toward their QD ground states. In this evolution of the carrier population, dephasing due to carrier scattering competes with the necessary buildup of excitonic correlations. It has been discussed for quantum wells in Ref. 26 that the formation process might take longer than the recombination process. For QDs, it has been shown in Ref. 18 that while electrons and holes are still localized by the strong confinement potential, excitonic correlations are easily suppressed by dephasing processes related to carrier scattering.

In general, the analysis leading to Eq. (6) has shown that the recombination dynamics is determined by (i) the electron and hole populations and (ii) the Coulomb correlations between the carriers. The high flexibility in fabricating self-assembled QDs allows us to tailor the corresponding parameters such that their impact can be systematically tested. In detail, the following experiments have been performed.

(i) The electron and hole populations have been varied by studying the carrier dynamics in undoped QDs in comparison to those in either *n*-type or *p*-type doped QDs.

(ii) Coulomb interaction can lead to carrier scattering between QD shells. The resulting dephasing can be enhanced by reducing the shell splitting. Therefore, the influence of correlations has been studied by addressing dots with different confinement heights.

(iii) By changing the photon energy of the exciting laser, we can distinguish between resonant excitation of the QD ground state for which the luminescence is studied, excitation of carriers in higher QD states, and above-barrier excitation in delocalized states. In the latter two cases, the carriers are incoherently generated. For above-barrier excitation, we expect, in general, a larger variety of possible carrier scattering channels.

A. Influence of excitation energy

First, we discuss the influence of the available excess energy on the exciton recombination dynamics. For that purpose, the excitation was decreased from being nonresonant into the GaAs barrier to being into the wetting layer, and further into the confined QD states. Figure 2 shows transients of the electron-hole recombination from the ground state of nominally undoped (In,Ga)As/GaAs QDs with a confinement potential of about 80 meV, i.e., the confinement potential in these dots is rather shallow. Note the logarithmic scale on the left axis. The excitation pulse hits the sample at time zero with a power of 8 W cm^{-2}. It is difficult to provide precise values for the average exciton population per dot. A rough estimate leads to 0.15 or below. Assuming a Poisson distribution, the probability of multiexciton generation under these circumstances is small. It might occur if a dark exciton has been formed after nonresonant excitation, which does not decay until one of the subsequent excitation events due to spin-flip suppression. If excited, a biexciton complex with an enhanced decay rate can be formed. From the weak dark exciton background, however, no strong contribution from such processes is expected. Our estimations are also supported by the purely exponential decay for resonant excitation (see below), which shows that biexcitonic involvements are weak.

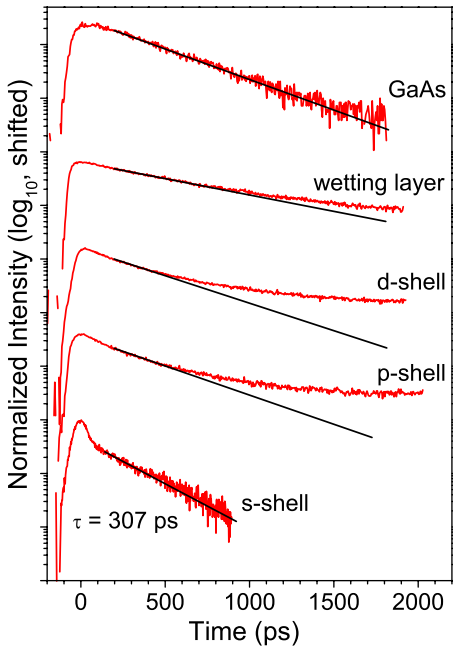

FIG. 2. (Color online) TRPL transients of undoped (In,Ga)As/GaAs self-assembled QDs with a confinement potential height of 80 meV. Pulsed excitation occurred at time zero. Detected was the ground state luminescence. The energy of the laser for GaAs, wetting layer, *d*-shell, *p*-shell, and *s*-shell excitation was set to 1.550, 1.476, 1.436, 1.414, and 1.389 eV respectively. The average excitation density was 8 W/cm^2. For resonant excitation, the signal is influenced by scattered laser light around time zero. $T = 10$ K. The lines are attempts to fit the data in a time range of 300 ps from 200 to 500 ps after the transient starts to show a clear decay. The decay times obtained in that way are 481, 685, 418, 337, and 307 ps from bottom to top with an error of about 20 ps.

The top trace shows the result for GaAs excitation. After a typical rise of the signal during a few tens of picoseconds, the intensity drops on a few hundred picosecond time scale. The solid line shows an attempt to fit a monoexponential decay to the data at early times. For the fit, a 300 ps range after the photoluminescence (PL) maximum has been used, in this case from 200 to 500 ps. After about a nanosecond, a deviation from this decay can be seen, as the data lie systematically above the experimental fit. This deviation becomes more pronounced for wetting layer excitation, for which already after 700 ps the nonexponential behavior of the decay becomes obvious. Note further that the rise time of the signal is reduced as compared to the case of GaAs excitation.

The nonexponential decay is also seen if the excitation is done below the barrier into the *d* shell or the *p* shell of the QDs, as demonstrated by the two mid traces. It has become even more pronounced than for above-barrier illumination,

as the deviation becomes apparent for delays as early as 500 ps. At these delays, the decay appears to be faster than for above-barrier excitation which might be related to a more rapid formation of optically active excitons in the ground state.

Note that these results for below-barrier excitation also indicate that the deviation from exponentiality cannot be traced to dark excitons, whose radiative decay requires a spin flip first. As soon as carriers are trapped in the QD ground states, spin relaxation is strongly suppressed at low T, in particular, because the spin-orbit coupling mechanisms which are very efficient in higher dimensional systems are strongly suppressed.[27,28] The resulting flip times are in the microsecond range and may even reach milliseconds,[29] which is by far too long to give any significant contribution to the decay dynamics in the monitored time range.

This is consistent with previous observation that the exciton spin-flip time exceeds tens of nanoseconds.[30] In the experiment here with a 75.6 MHz laser repetition rate, a dark exciton contribution would appear as constant background at the low temperatures applied. Any such background related to dark excitons (or also due to noise) has been subtracted and therefore does not affect the decay analysis. As compared to maximum intensity, this background has an intensity in the percent range. When the laser repetition rate is reduced, a slowly decaying background can be resolved for delays exceeding 10 ns, at which all recombination processes involving optically active carriers occurred.

Increasing the excitation power in the regime where multiexciton effects are negligible leads also to slight variations of the decay dynamics: For excitation into the barrier, the decay tends to be slowed down in the range of 10%, which might be attributed to enhanced carrier diffusion before trapping into the QD. For excitation into higher lying QD states, the changes are weak, when varying the excitation power. Note also that we do not observe significant variations of the decay time across the QD emission band, irrespective of the excitation energy.

The bottom trace of Fig. 2, finally, shows the TRPL for resonant excitation between the valence and conduction band ground states. Around zero delay, scattered light from the laser is seen. After ~50 ps, a decay becomes prominent, which is purely exponential within the experimental accuracy, in contrast to the previous nonresonant excitation conditions. Furthermore, the decay is much faster than before. Comparing the decay time to those determined by fitting the early times data under nonresonant conditions, we find an acceleration from 481 ps (685 ps) for GaAs (wetting layer) excitation to 307 ps for resonant excitation. For nonresonant excitation, the optically excited polarization is converted into populations by the scattering involved in the relaxation. For resonant excitation, on the other hand, the carrier coherence is maintained until recombination occurs, as recent four-wave-mixing studies have demonstrated.[1] Therefore, under these conditions, coherently driven luminescence is observed. Corresponding calculations are very involved as they require additional inclusion of interband coherence terms in the dynamics. However, from the theory in the incoherent regime, we expect strong carrier correlations for resonant excitation, i.e., for the source term of spontaneous emission,

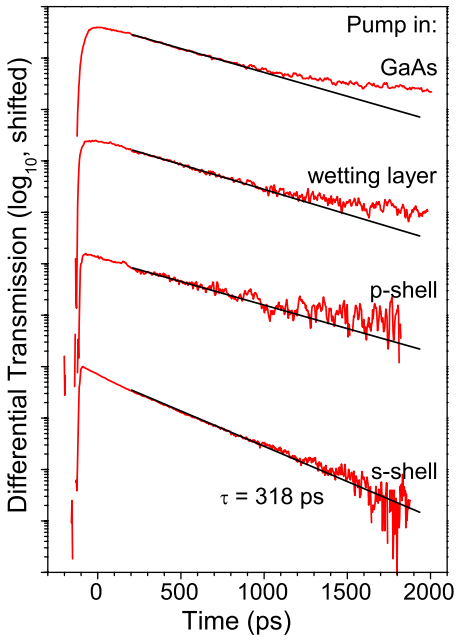

FIG. 3. (Color online) TRDT transients of the (In,Ga)As/GaAs self-assembled QDs with a confinement potential height of 80 meV studied also in Fig. 2. The ground state populations were probed for different excitation energies of the pump laser, which for GaAs, wetting layer, p-shell, and s-shell excitation were the same as in the TRPL experiments. The average pump (probe) density was 0.7 W/cm^2 (0.07 W/cm^2). T=10 K. The lines are linear fits to the data in the time range from 200 to 500 ps, giving decay times of 540, 467, 367, and 318 ps from bottom to top with 20 ps accuracy. Note that the resonant excitation value is the same as for resonant PL.

we have $f^e f^h + C^x \approx f^e$. Hence, since $f^e > f^e f^h$, Eq. (6) predicts a faster decay for resonant excitation. The comparatively short exciton lifetime as compared to standard self-assembled QDs[5] arises from the large dot volume, which determines the exciton coherence volume and therefore its oscillator strength.

The TRPL results are confirmed by the TRDT studies shown in Fig. 3. The energy of the pump beam was tuned in the same way as in the TRPL studies described above. The energy of the probe was fixed to the s shell. The shapes of the different traces are similar to those observed in TRPL. For excitation into GaAs, the transmission clearly deviates from an exponential decay, and the same is true for excitation into the wetting layer, the d shell (not shown, very similar to the p shell case) and the p shell. In contrast, for resonant excitation, an exponential decay is observed again with a characteristic time significantly shorter than that for nonresonant excitation and identical to the one in the TRPL studies.

Note that the contributions of optically active electron-hole configurations and optically inactive carrier populations enter differently in TRPL and TRDT (see Sec. II). Therefore, the decay curves cannot be directly compared to each other in case of nonresonant excitation. The formation of inactive excitons is related to spin-flip processes, which are most efficient for above-barrier excitation. Therefore, we expect a

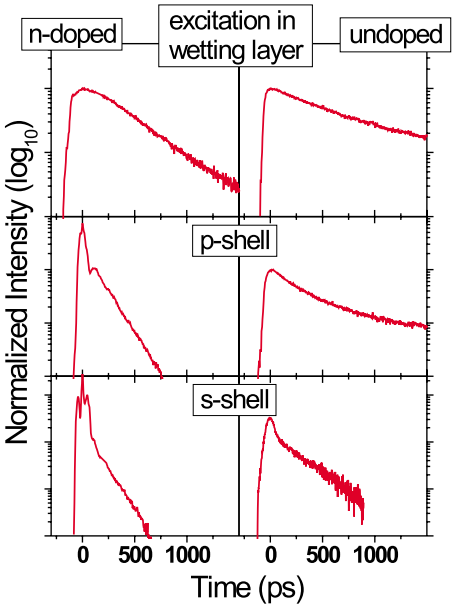

FIG. 4. (Color online) Comparison of TRPL traces for *n*-doped (left panels) and undoped (right panels) QDs excited at different energies. The excitation energy for the *n*-doped sample in wetting layer, *p* shell, and *s* shell was set to 1.550, 1.417, and 1.397 eV, respectively. The height of the confinement potential is about 80 meV. Around time zero, the signal is influenced by scattered laser light. $T=10$ K. The average excitation density was 8 W/cm^2.

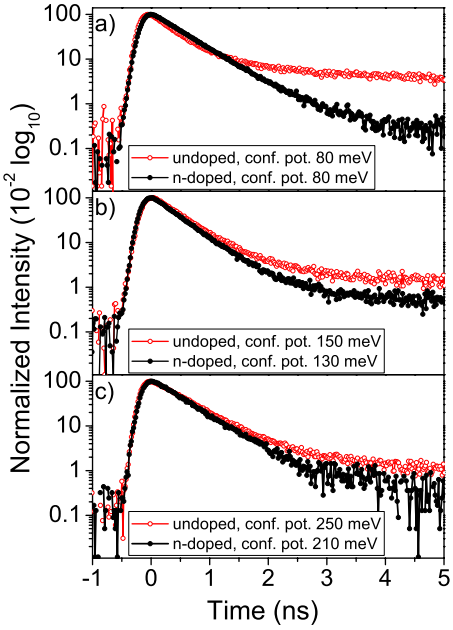

FIG. 5. (Color online) TRPL transients for undoped (open symbols) and *n*-doped (full symbols) QDs with different confinement potentials, as indicated in each panel. Excitation was done into GaAs at 1.550 eV. $T=10$ K. The excitation density was 8 W/cm^2.

considerable difference between TRPL and TRDT for nonresonant excitation into GaAs, as confirmed by comparison of Figs. 2 and 3. In contrast, for below-barrier excitation, the difference appears to be reduced.

B. Influence of doping

Neglecting the influence of correlations between electrons and holes, described by C^x in Eq. (6), the carrier population dynamics can be pushed toward a monoexponential decay if either the electron or the hole population is approximately held constant. This can be achieved by a background doping when the population due to doping is larger than the pump-induced population. The doping carriers would also serve as a source for strong dephasing that rapidly diminishes C^x. We studied both *n*- and *p*-doped samples which were prepared such that there is on average a single carrier per dot. The studies show that besides variations in the quantitative values for the decay times, the shape is very similar, independent of the type of doping. Therefore, we focus on the *n*-doped structures only.

Figure 4 depicts the corresponding TRPL results for *n*-doped QDs, excited at different energies. The confinement potential was about 80 meV. For comparison, the data for the undoped dots from Fig. 2 are also shown. Clearly, the decay behavior of the doped dots comes much closer to an exponential decay, independent of the actual excitation energy. For wetting layer excitation, the decay deviates more strongly from the exponential shape in the undoped case. More clearly visible for *p*-shell excitation, the undoped QDs show a nonexponential decay, while the doped QDs follow already to a good approximation an exponential decay dynamics. For resonant excitation, monoexponential decays are seen in both cases.

Note that we cannot fully exclude that the deviation from exponentiality for the *n*-doped QDs under above-barrier excitation results at least partly from contributions due to charge neutral QDs. The nonresonant excitation can lead to a depletion of charges from the doping. Vice versa, for nominally undoped QDs, the above-barrier excitation can also lead to formation of charged excitons. As for charged dots, the decay comes closer to an exponential behavior; this gives a hint why the PL decay in the undoped QDs is closer to an exponential behavior for excitation into GaAs than for wetting layer excitation. On the other hand, formation of charged exciton complexes is strongly suppressed for below-barrier excitation.

C. Influence of correlations

The magnitude of the correlations between carriers due to Coulomb interactions can be tailored by varying the QD confinement. With increasing confinement potential, the splitting between the dot shells increases, while possible scattering (that suppresses correlations) is reduced. This was studied by comparing QDs annealed at different temperatures. Figure 5 shows the results for QD samples which were excited nonresonantly into GaAs. For comparison, again the data for undoped and *n*-doped QDs are displayed. The height of the confinement potentials increased from 80 (80) to 150 (130) and further to 250 (210) meV for the undoped (*n*-doped) structures. The resulting splittings between the confined QD shells, as estimated from high excitation PL spectroscopy, are 20, 35, and 50 meV, respectively.

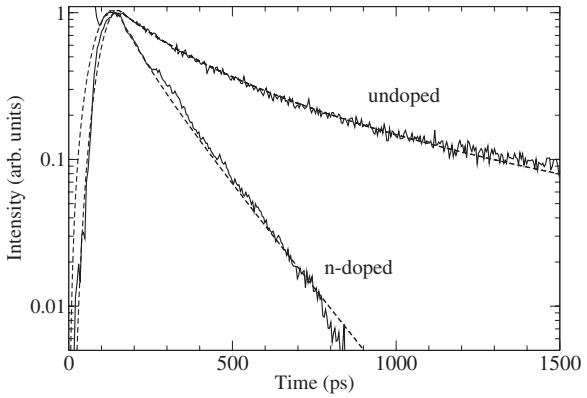

FIG. 6. Calculated TRPL intensity (dashed lines) according to Eq. (1) for pumping into the p shell of undoped and n-doped QDs. The experimental data (solid lines) are the same as in Fig. 4.

In all cases, it can be seen that the dynamics in the undoped dots deviates more strongly from an exponential decay than that in the doped structures. However, with increasing confinement, the difference becomes smaller, and for the strongest confinement, the traces almost coincide. In this particular case, the influence of the Coulomb scattering has been reduced to an extent that it is no longer relevant for the dephasing of correlations.

V. NUMERICAL RESULTS

In this section, we provide exemplary numerical results which support the previous conclusions. The semiconductor luminescence equations are used to describe the time evolution of the photon number $\langle b_\xi^\dagger b_\xi \rangle$, the carrier populations $f_\nu^{(e,h)}$, the photon-assisted polarization $\langle b_\xi^\dagger h_\nu e_\nu \rangle$, and the carrier-carrier correlations such as $C^x_{\alpha\nu\alpha\nu} = \delta \langle e_\alpha^\dagger e_\nu h_\alpha^\dagger h_\nu \rangle$. Scattering is treated in relaxation-time approximation. We restrict ourselves to the formulation of the theory in the incoherent regime, as presented in Ref. 18, and consider nonresonant excitation. The QD parameters are those used in Ref. 18, except that the QD density is $N = 10^{10}$ cm^{-2}, the dipole moment is 16.8 e Å, and the dephasing of the correlations is 0.05 meV. Even though the dephasing is weak, it efficiently destroys the correlations on a time scale of tens of picoseconds.

Figure 6 shows results for undoped and n-doped QDs excited in the p shell. For the undoped situation, we pump the system with equal electron and hole densities $N_e = N_h = 0.35N$. In the n-doped case, we assume on average one additional electron per QD, i.e., $N_e = N_h + N$ with again $N_h = 0.35N$. Apart from this difference in the initial conditions, both curves have been calculated with exactly the same parameters. A reasonable agreement between theory and experiment can be observed: (i) The doped QDs show an exponential decay, whereas the undoped ones show a nonexponential decay. (ii) The decay is much faster for the doped QDs if compared to the undoped QDs. Simply speaking, this difference comes from the enhanced availability of carriers in the doped QD ground states, as either the resident electron or the optically excited one can contribute.

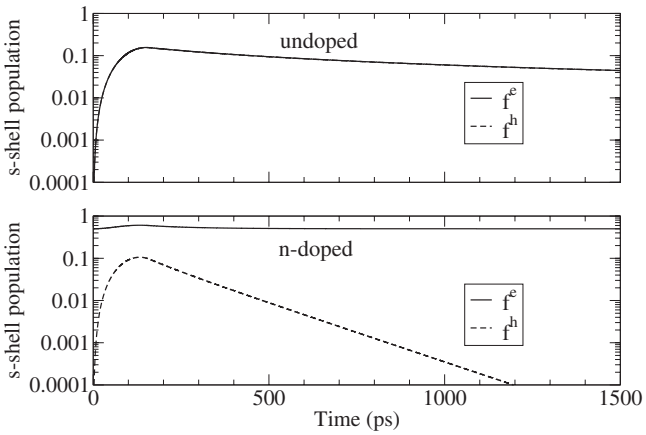

FIG. 7. Time evolution of electron and hole populations, f^e and f^h, in the s shell of undoped (top) and n doped (bottom) QDs. The population is to be understood per spin degree of freedom, i.e., an s-shell population of unity corresponds to the occupation by two carriers with opposite spins, while a value of 0.5 corresponds to an occupation by a single carrier.

To understand the origin of these different behaviors, it is illuminating to study the time evolution of the s-shell populations, as depicted in Fig. 7 for one spin subsystem. In the undoped case, the s-shell populations are zero at first. Due to the pump process and the subsequent carrier scattering, the s-shell population increases temporarily and decays subsequently to its initial value. In the n-doped case, the electron occupation in the s shell starts with the finite value of 0.5 due to the doping. The temporal change of the electron population relative to the doping level is small. According to Eq. (6), a constant electron population f_α^e leads to an exponential decay of the hole population f_α^h and, hence, of the PL intensity for the considered situation of strong suppression of excitonic correlations C^x due to dephasing.

VI. CONCLUSIONS

In summary, we have performed a detailed study of the carrier recombination dynamics in QDs. The results show that the carrier recombination, in general, follows a nonexponential decay. Only under specific conditions, like resonant excitation, strong confinement, or intentional doping, is a monoexponential decay observed. In addition, ensuring coherence of the excited carriers by resonant excitation leads to a strong shortening of the decay time. The experimental results are in agreement with numerical results obtained from a microscopic theory which abandons the shortcomings of the commonly used two-level description of QDs.

ACKNOWLEDGMENTS

We gratefully acknowledge the financial support of this work by the Deutsche Forschungsgemeinschaft (research group "Quantum Optics in Semiconductor Nanostructures" and the Research Project No. BA 1549/10-1). The Bremen group acknowledges a grant for CPU time at the NIC, Forschungszentrum Jülich.

[1] W. Langbein, P. Borri, U. Woggon, V. Stavarache, D. Reuter, and A. D. Wieck, Phys. Rev. B **70**, 033301 (2004).
[2] P. Michler, A. Imamoglu, M. D. Mason, P. J. Carson, G. F. Strouse, and S. K. Buratto, Nature (London) **406**, 968 (2000).
[3] S. Stufler, P. Ester, A. Zrenner, and M. Bichler, Phys. Rev. B **72**, 121301(R) (2005).
[4] See, for example, P. Borri, W. Langbein, S. Schneider, U. Woggon, R. L. Sellin, D. Ouyang, and D. Bimberg, Phys. Rev. Lett. **87**, 157401 (2001); M. Bayer and A. Forchel, Phys. Rev. B **65**, 041308(R) (2002).
[5] See, for example, W. Yang, R.-R. Lowe-Webb, H. Lee, and P. C. Sercel, Phys. Rev. B **56**, 13314 (1997); S. Raymond, S. Fafard, P. J. Poole, A. Wojs, P. Hawrylak, S. Charbonneau, D. Leonard, R. Leon, P. M. Petroff, and J. L. Merz, *ibid.* **54**, 11548 (2005); F. Adler, M. Geiger, A. Bauknecht, D. Haase, P. Ernst, A. Dörnen, F. Scholz, and H. Schweizer, J. Appl. Phys. **83**, 1631 (1998).
[6] J. Hours, P. Senellart, E. Peter, A. Cavanna, and J. Bloch, Phys. Rev. B **71**, 161306(R) (2005).
[7] A. Melliti, M. A. Maaref, F. Hassen, M. Hjiri, H. Maaref, J. Tignon, and B. Sermage, Solid State Commun. **128**, 213 (2003).
[8] V. Zwiller, M. E. Pistol, D. Hessman, R. Cederström, W. Seifert, and L. Samuelson, Phys. Rev. B **59**, 5021 (1999).
[9] F. Adler, M. Geiger, A. Bauknecht, F. Scholz, H. Schweizer, M. H. Pilkuhn, B. Ohnesorge, and A. Forchel, J. Appl. Phys. **80**, 4019 (1996).
[10] R. A. Oliver, G. Andrew, D. Briggs, M. J. Kappers, C. J. Humphreys, J. H. Rice, J. D. Smith, and R. A. Taylor, Appl. Phys. Lett. **83**, 755 (2003).
[11] O. Labeau, P. Tamarat, and B. Lounis, Phys. Rev. Lett. **90**, 257404 (2003).
[12] I. L. Krestnikov, N. N. Ledentsov, A. Hoffmann, D. Bimberg, A. V. Sakharov, W. V. Lundin, A. F. Tsatsul'nikov, A. S. Usikov, Zh. I. Alferov, Yu. G. Musikhin, and D. Gerthsen, Phys. Rev. B **66**, 155310 (2002).
[13] B. V. Kamenev, J.-M. Baribeau, D. J. Lockwood, and L. Tsybeskov, Physica E (Amsterdam) **26**, 174 (2005).
[14] A. S. Dissanayake, J. Y. Lin, and H. X. Jiang, Phys. Rev. B **51**, 5457 (1995).
[15] Yu-Shen Yuang, Yang-Fang Chen, Yang-Yao Lee, and Li-Chi Liu, J. Appl. Phys. **76**, 3041 (1994).
[16] V. Türck, S. Rodt, O. Stier, R. Heitz, R. Engelhardt, U. W. Pohl, D. Bimberg, and R. Steingruber, Phys. Rev. B **61**, 9944 (2000).
[17] B. Patton, W. Langbein, and U. Woggon, Phys. Rev. B **68**, 125316 (2003).
[18] N. Baer, C. Gies, J. Wiersig, and F. Jahnke, Eur. Phys. J. B **50**, 411 (2006).
[19] T. R. Nielsen, P. Gartner, and F. Jahnke, Phys. Rev. B **69**, 235314 (2004).
[20] J. Seebeck, T. R. Nielsen, P. Gartner, and F. Jahnke, Phys. Rev. B **71**, 125327 (2005).
[21] C. Gies, J. Wiersig, M. Lorke, and F. Jahnke, Phys. Rev. A **75**, 013803 (2007).
[22] S. M. Ulrich, C. Gies, S. Ates, J. Wiersig, S. Reitzenstein, C. Hofmann, A. Löffler, A. Forchel, F. Jahnke, and P. Michler, Phys. Rev. Lett. **98**, 043906 (2007).
[23] J. Fricke, Ann. Phys. (N.Y.) **252**, 479 (1996).
[24] M. Schwab, H. Kurtze, T. Auer, T. Berstermann, M. Bayer, J. Wiersig, N. Baer, C. Gies, F. Jahnke, J. P. Reithmaier, A. Forchel, M. Benyoucef, and P. Michler, Phys. Rev. B **74**, 045323 (2006).
[25] A. Greilich, M. Schwab, T. Berstermann, T. Auer, R. Oulton, D. R. Yakovlev, M. Bayer, V. Stavarache, D. Reuter, and A. Wieck, Phys. Rev. B **73**, 045323 (2006).
[26] W. Hoyer, M. Kira, and S. W. Koch, Phys. Rev. B **67**, 155113 (2003).
[27] A. V. Khaetskii, D. Loss, and L. Glazman, Phys. Rev. Lett. **88**, 186802 (2002); I. A. Merkulov, Al. L. Efros, and M. Rosen, Phys. Rev. B **65**, 205309 (2002); R. de Sousa and S. Das Sarma, *ibid.* **67**, 033301 (2003); L. M. Woods, T. L. Reinecke, and Y. Lyanda-Geller, *ibid.* **66**, 161318 (2002); L. M. Woods, T. L. Reinecke, and R. Kotlyar, *ibid.* **69**, 125330 (2004).
[28] T. Brandes and T. Vorrath, Phys. Rev. B **66**, 075341 (2002); V N. Golovach, A. Khaetskii, and D. Loss, Phys. Rev. Lett. **93**, 016601 (2004); R. Hanson, B. Witkamp, L. M. K. Vandersypen, L. H. Willems van Beveren, J. M. Elzerman, and L. P. Kouwenhoven, *ibid.* **91**, 196802 (2003).
[29] See, for example, M. Kroutvar, Y. Ducommun, D. Heiss, M. Bichler, D. Schuh, G. Abstreiter, and J. J. Finley, Nature (London) **432**, 81 (2004).
[30] M. Paillard, X. Marie, P. Renucci, T. Amand, A. Jbeli, and J. M. Gérard, Phys. Rev. Lett. **86**, 1634 (2001).